

# Band structure in classical field theory

Michael Salem and Tanmay Vachaspati  
*Department of Physics, Case Western Reserve University,  
 10900 Euclid Avenue, Cleveland, OH 44106-7079, USA.*

Stability and instability bands in classical mechanics are well-studied in connection with systems such as described by the Mathieu equation. We examine whether such band structure can arise in classical field theory in the context of an embedded kink in 1+1 dimensions. The static embedded kink is unstable to perturbations but we show that if the kink is dynamic it can exhibit stability in certain parameter bands. Our results are relevant for estimating the lifetimes of various embedded defects and, in particular, loops of electroweak Z-string.

PACS numbers: 98.80.Cq

## I. INTRODUCTION

A wide variety of classical static solutions in field theories have been constructed and they can play crucial roles in particle physics, condensed matter systems, and cosmology. Commonly the static solutions exist because of non-trivial topology of the field theory and in these cases the solution is known as a “topological defect”. Alternately the solution may exist in the form of a topological defect embedded in a theory where the requisite topology is absent. In these cases the static embedded topological defect is usually unstable and can decay. We are interested in determining if this instability is also present in embedded defects that are not static.

It is helpful to consider a mechanical analog of the unstable defect solution. Consider a particle in two spatial dimensions with position  $\mathbf{x}(t) = (x(t), y(t))$  and Lagrangian

$$L = \frac{1}{2}m\mathbf{v}^2 - V(\mathbf{x}) \quad (1)$$

where

$$V(\mathbf{x}) = \frac{k_x}{2}x^2 - \frac{k_y}{2}y^2 + \frac{c}{2}x^2y^2 \quad (2)$$

with  $k_x$ ,  $k_y$  and  $c$  being positive parameters. The extremum of the potential is at  $\mathbf{x} = 0$  and is a saddle point. The positive eigenvalue at the saddle point is along the  $x$  direction and the negative eigenvalue is along the  $y$  direction. The equations of motion are:

$$m\ddot{x} = -k_x x - cx y^2 \quad (3)$$

$$m\ddot{y} = +k_y y - cx^2 y \quad (4)$$

where overdots denote derivatives with respect to  $t$ . The static solution is  $x = 0 = y$  and is clearly unstable to perturbations in the  $y$  direction. This is seen by taking  $y$  to be a perturbation and then linearizing the equation for  $y$ :

$$m\ddot{y} = +k_y y \quad (5)$$

This equation has exponentially growing solutions and hence the particle is unstable to “rolling off” in the  $y$ -direction.

Next consider a dynamic solution of the system:

$$x(t) = A \cos(\omega t), \quad y(t) = 0 \quad (6)$$

where  $\omega = \sqrt{k_x/m}$ . Is this solution stable?

Once again we proceed by perturbing the  $y$  equation, and linearizing in the perturbations. This gives

$$m\ddot{y} = +k_y y - cA^2 \cos^2(\omega t)y \quad (7)$$

where  $y$  denotes the perturbation. This is the Mathieu equation (Sec. 5.2, [1]).

There exist solutions to the Mathieu equation of the form

$$y(t) = e^{i\nu t} P(t), \quad (8)$$

a result which is derived using Floquet’s theorem. The value of  $\nu$  depends on the parameters  $k_y/k_x$  and  $cA^2/k_x$  and can be found as described in Sec. 5.2 of Ref. [1]. If  $\nu$  is imaginary, the original solution is unstable; if  $\nu$  is real, the original solution is stable.

A remarkable feature of this system is that there are bands of stability and instability. For fixed  $\omega$ , if  $A$  is close to zero, there is an instability and the particle rolls off in the  $y$ -direction. For larger  $A$ , we find stability – the particle gets displaced in the  $y$ -direction at the saddle point, but is unable to roll off by the time it has moved away from the saddle point in the  $x$ -direction. This is shown in Fig. 1 where we have plotted the stability and instability bands in the  $a - q$  plane, where

$$a = \frac{cA^2}{2k_x} - \frac{k_y}{k_x}, \quad q = -\frac{cA^2}{4k_x}. \quad (9)$$

Then, for fixed  $k_y/k_x$ , we get the line

$$a = -2q - \frac{k_y}{k_x} \quad (10)$$

on the plot. This line intersects the unstable and stable regions alternately as we go to larger amplitudes for fixed model parameters.

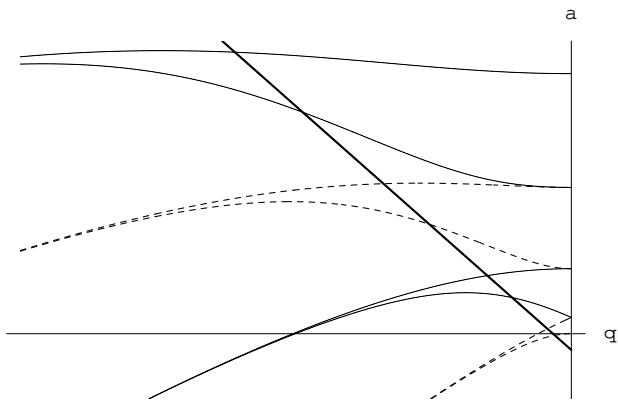


FIG. 1: Band structure for the Mathieu equation. For  $q < 0$ , the stability bands lie between consecutive dashed or consecutive solid curves. The straight line denotes a set of parameters for the mechanical model for different values of the oscillation amplitude. Larger amplitudes correspond to points on the line that are further away from the origin. As the amplitude is increased, the line increasingly lies in the stability bands but no matter how large the amplitude, there are always bands where there is instability.

It is tempting to think that the pattern of stability and instability as the amplitude is increased can be understood in terms of the time spent by the particle in the vicinity of the saddle point as compared to the decay time of the static solution. However, this intuition does not work since for yet larger  $A$  we again get instability. The band structure then has to be understood as a resonance phenomenon between the various oscillatory modes of the particle.

If we include frictional forces on the particle as it moves on the potential, the amplitude of oscillations will gradually diminish and eventually the particle will enter a band of instability. The decay time of the oscillations will then be determined by the time it takes for the particle to slip from a stability band to an instability band.

We are interested in determining if a similar phenomenon can occur in classical field theories. If a certain static field solution is unstable, can its lifetime be much longer due to some dynamics? There is clearly an affirmative though trivial answer – since these are relativistic field theories, a boosted field solution lives longer due to relativistic time dilation. However, we are not interested in this factor and would like to determine if there is an effect similar to the band structure observed in the mechanical problem. There is another complication in field theory: the dynamical solution will almost certainly emit radiation and dissipate and hence is similar to the mechanical case with the inclusion of friction. Yet in the examples we will consider, the dissipation due to radiation is very small and can be ignored.

We will restrict our attention in this paper to classical field theory in 1+1 dimensions. Our first approach to the problem is to construct unstable (embedded) kink solutions and study the growth of linearized perturbations on

kink solutions that are forced to oscillate. The similarity between this field theory problem and the mechanical problem described above can be understood by going to the rest frame of the kink as it oscillates. In this (non-inertial) frame the perturbation modes are oscillating in the vicinity of the kink. In the time when a perturbation mode lies outside the kink, it cannot grow. The mode can only grow during the time that it lies within the kink. This is exactly like the mechanical model where the particle (analogous to the perturbation mode) can roll off in the  $y$ -direction near the saddle point but not when its oscillations take it away from  $x = 0$ . Hence we expect the behaviour of the perturbation mode to be similar to that of the particle.

Indeed our analysis reveals band structure in the growth of the perturbation modes though we only find stability when the amplitude of the kink oscillations is comparable to the width of the kink. In other words, in the linearized analysis only “jittering” kink backgrounds are found to have stability bands. We have also performed a second analysis of the problem. In this approach, we impose an external potential in which the kink can oscillate. Now we evolve the full field equations and find the lifetime of the kink. Here again we find band structure. Furthermore, the amplitude of motion can be significantly larger than the kink width. We attribute the enhanced stability bands at large amplitudes to the reduced and varying kink width in the external potential.

Our study has obvious implications for the study of classical solutions that are unstable when static. Examples of such solutions include a variety of embedded defects [2, 3]. In particular, electroweak Z-strings are an important example [4, 5]. Assuming, for now, that the band structure exists for dynamical solutions in 3+1 dimensions as well, we discuss the possible relevance of our work to the electroweak model in Sec. IV.

## II. LINEARIZED ANALYSIS OF FIELD THEORY PROBLEM

The 1+1 dimensional field theory we choose to study is one that contains embedded kink solutions [2, 3]. The complex scalar field,  $\phi = \phi_1 + i\phi_2$ , has the Lagrangian density:

$$L = \frac{1}{2} |\partial_\mu \phi|^2 - V(\phi) \quad (11)$$

where

$$V(\phi) = \frac{1}{4} (|\phi|^2 - 1)^2 + \frac{(c-1)}{2} \phi_1^2 \phi_2^2. \quad (12)$$

(In 1+1 dimensions, the fields are dimensionless. For convenience, we have also rescaled the coordinates so that they are dimensionless.) The last term in the potential is analogous to the cross-term in eq. (2) and it violates the  $U(1)$  symmetry  $\phi \rightarrow \exp(i\alpha)\phi$  when  $c \neq 1$  but preserves a  $Z_2 \times Z_2$  subgroup. A vacuum expectation value of either

the real ( $\phi_1$ ) or imaginary component ( $\phi_2$ ) of  $\phi$  spontaneously breaks the symmetry to the identity group. Hence there are topological kink solutions in the model for  $c \neq 1$ . However, we will not be interested in these topological solutions. Instead we will study the embedded kink solution which is not topological and exists for all values of  $c$ . This solution is:

$$\phi_1 = \tanh\left(\frac{x}{\sqrt{2}}\right), \quad \phi_2 = 0 \quad (13)$$

In the sub-space of field configurations defined by  $\phi_2 = 0$ , the embedded kink is topological and hence stable. However, in the full field space, the static embedded kink is unstable to perturbations in the  $\phi_2$  direction. The equation for linearized perturbations in the  $\phi_2$  direction in the static embedded kink background is:

$$\ddot{\phi}_2 - \phi_2'' + (c\phi_1^2 - 1)\phi_2 = 0 \quad (14)$$

where  $\phi_1$  is given in eq. (13). The solution for  $\phi_2$  is a hypergeometric function (Sec. 6.3, [1]):

$$\phi_2 = e^{i\nu t} \text{sech}^K\left(\frac{x}{\sqrt{2}}\right) F\left(K + \frac{1}{2} + P, K + \frac{1}{2} - P | K + 1 | z\right) \quad (15)$$

with

$$z = \frac{1}{2} \left[ 1 + \tanh\left(\frac{x}{\sqrt{2}}\right) \right], \quad (16)$$

$$K^2 = 2(c - 1 - \nu^2), \quad (17)$$

$$P = \sqrt{2c + \frac{1}{4}}. \quad (18)$$

The lowest eigenvalue  $\nu_0$  is given by:

$$\nu_0^2 = \frac{1}{2} \sqrt{2c + \frac{1}{4}} - \frac{5}{4} \quad (19)$$

Since  $\nu_0$  is imaginary for  $1 \leq c < 3$ , the static solution in eq. (13) is unstable for these parameter values. For  $c = 3$ , the lowest value of  $\nu$  is zero, corresponding to the translation mode of the topological  $Z_2$  kink [6]. Hence for  $c \geq 3$ , the static embedded kink is stable.

We now want to introduce some dynamics to the embedded kink solution and study the effect of the dynamics on the unstable mode in the  $\phi_2$  direction. In the linearized approach to the problem, the dynamics is introduced “by hand” by introducing a time dependence in the unperturbed background:

$$\phi_1 = \tanh\left[\frac{\gamma}{\sqrt{2}}(x - g(t))\right], \quad \phi_2 = 0 \quad (20)$$

where

$$g(t) = A \cos(\omega t) \quad (21)$$

describes oscillations with amplitude  $A$  and angular frequency  $\omega$ , and  $\gamma$  is the “Lorentz factor”

$$\gamma = \frac{1}{\sqrt{1 - \dot{g}^2}} \quad (22)$$

We require  $\omega A < 1$  so that the speed of the kink is always sub-luminal. In this background the equation for  $\phi_2$  perturbations is:

$$\ddot{\phi}_2 - \phi_2'' + (c \tanh^2 X - 1)\phi_2 = 0 \quad (23)$$

where

$$X(t, x) \equiv \frac{\gamma}{\sqrt{2}}(x - g(t)). \quad (24)$$

Note that boosts of the static solution can be obtained by setting  $g = vt$  where  $v$  is the speed of the kink. Such backgrounds do have a longer lifetime but this is due to the special relativistic time dilation.

In Appendix A we extend Floquet’s theorem to field theory to show that solutions of eq. (23) have the form:

$$\phi_2(t, x) = e^{i\nu t} P(t, x) \quad (25)$$

where  $P(t, x)$  is a periodic function in  $t$ :

$$P(t + 2\pi\omega^{-1}, x) = P(t, x)$$

The next step is to find the eigenvalue  $\nu$ . We were unable to determine  $\nu$  analytically and instead solved eq. (23) numerically for various parameters  $A$ ,  $\omega$  and  $c$  and with an initial perturbation:

$$\phi_2(t = 0, x) = \text{sech}(X(0, x)) \quad (26)$$

A sample result of the numerical evolution is shown in Fig. 2. Here we plot  $P(t, x)$  for several different values of  $X$  (see eq. (24)) versus time. The plots are consistent with the form in eq. (25). For some values of  $A$ ,  $\phi_2(t, x)$  grows exponentially with time, while for others it oscillates without growth. This allows us to find the lifetime,  $\tau$ , of the background. In Fig. 3, we show the inverse lifetime,  $\tau^{-1}$ , as a function of the amplitude  $A$  for  $c = 1, 2, 2.5$  with  $\omega$  fixed by the relation  $\omega = 0.99/A$ . The reason we held  $\omega = 0.99/A$  is that we expect that stability will depend on the acceleration  $a_c$  of the kink and this is  $\leq \omega^2 A$ . Since the speed cannot exceed the speed of light, we impose  $\omega A \leq 1$ . Therefore  $a_c \leq v_{max}^2/A$  where  $v_{max} = \omega A$  is the maximum speed of the kink. So we expect greatest stability when  $v_{max} \sim 1$  and for small oscillation amplitude. In Fig. 2, the bands of stability occur where the inverse lifetime vanishes.

It is worth noting that the values of  $A$  for which stability can occur are of order the half-width of the kink which is given by  $\sqrt{2}$ . Hence, stability bands only occur when the background is undergoing a rigid jittering

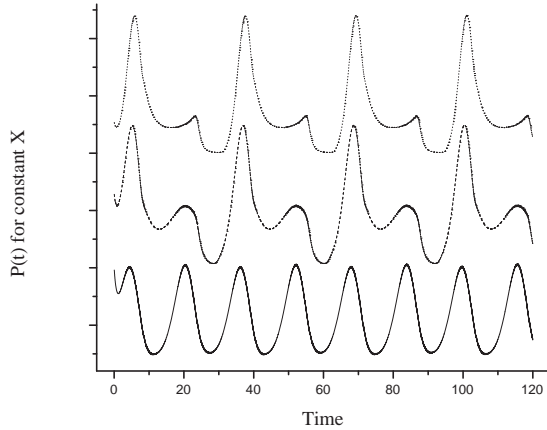


FIG. 2: The spatial value of the function  $P(t, x)$  for  $X = 0$  (solid curve), 1 (dashed curve), 2 (dotted curve) as a function of time.

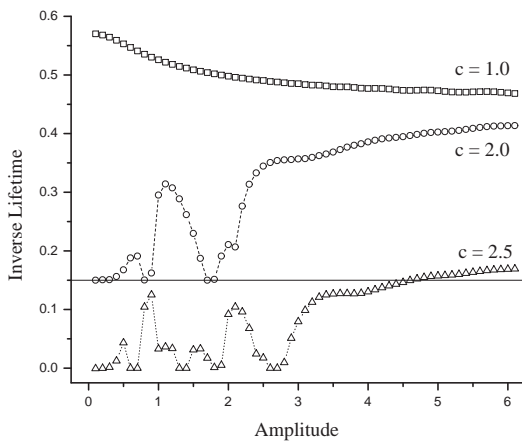


FIG. 3: The decay rate  $\tau^{-1}$  is plotted versus the amplitude of oscillation for  $c = 1$  (solid curve), 2 (dashed curve), and 2.5 (dotted curve), as determined in the linearized analysis. Stability bands are regions where  $\tau^{-1} = 0$ . There are no stability bands for  $c = 1$  but these do exist for  $c = 2$  and 2.5. The curve for  $c = 2$  has been off-set by 0.15 along the y-axis for clarity.

motion. The point  $A = 0$  is a singular point in our approach since the oscillation frequency is  $\omega = 0.99/A$  and this becomes infinite as  $A$  tends to zero. Another important point is that there are no stability bands for the embedded kink in the  $U(1)$  model obtained with  $c = 1$ . We also observe that the dynamic kink with  $c > 3$  can show instability. This is not inconsistent with our earlier analysis of the static kink – only the static kink is stable for  $c \geq 3$  and there is no reason why rigidly moving dynamic kinks should be stable when  $c \geq 3$ .

### III. FIELD THEORETIC PROBLEM WITH EXTERNAL POTENTIAL

A drawback of the linearized analysis is that it keeps the background “rigid” – the profile function is always a hyperbolic tangent – while an oscillating kink should also experience some profile fluctuations and be more like a “fluid”. Hence in our second analysis of the problem we treat the full field theory, rather than perform a perturbative analysis about a chosen field background. To obtain a dynamic embedded kink, we have introduced a background potential in which the embedded kink can oscillate. The Lagrangian density now is given by eq. (11) together with an additional “external” term in the potential:

$$V_{ext}(\phi) = \frac{1}{2}U(x)(\phi_1^2 - 1)^2 \quad (27)$$

where  $U(x)$  is a potential well in which the embedded kink oscillates. The external potential can possibly originate due to the expectation value of other very massive fields on which backreaction is unimportant<sup>1</sup>. A simple example for the external potential is  $U(x) = dx^2/2$  ( $d > 0$ ). Then  $V_{ext}$  provides a force between the position of the embedded kink (inside which  $\phi_1 \sim 0$ ) and the origin of the coordinate system ( $x = 0$ ). Hence an embedded kink that is initially displaced from  $x = 0$ , oscillates about  $x = 0$  and the frequency of oscillation is determined by the parameter  $d$ . In our numerical analysis, we have chosen

$$U(x) = \frac{d}{2}\alpha^2(1 - e^{-(x/\alpha)^2}) \quad (28)$$

and we have chosen  $\alpha = 15$ ,  $d = 0.1$ . Then  $U(x)$  has the  $x^2$  form for small  $x$  and changes to a constant for  $x \gg \alpha$ . The feature that  $U(x)$  does not diverge at large  $x$  has the advantage that radiation of  $\phi_1$  waves from the oscillating kink can escape to infinity.

Now the equations of motion for  $\phi_1$  and  $\phi_2$  are:

$$\ddot{\phi}_1 - \phi_1'' + (\phi_1^2 + c\phi_2^2 - 1)\phi_1 + 2U(\phi_1^2 - 1)\phi_1 = 0 \quad (29)$$

$$\ddot{\phi}_2 - \phi_2'' + (c\phi_1^2 + \phi_2^2 - 1)\phi_2 = 0. \quad (30)$$

The equations of motion are first solved numerically with the initial condition:

$$\phi_1(t = 0, x) = \tanh(\bar{X}(0, x)), \quad \phi_2(t = 0, x) = 0. \quad (31)$$

<sup>1</sup> This could be realized physically in a system which has a phase containing only unstable kinks (call it the A phase) that is sandwiched between layers of another phase (call it the B phase) in which the kinks are stable. Then the B-phase stable kink could be driven to oscillate across a region of A-phase where it would be unstable. The potential  $V_{ext}$  contains both the driving potential ( $U(x)$ ) and also the spatial variation of the phases because of the field dependence in it.

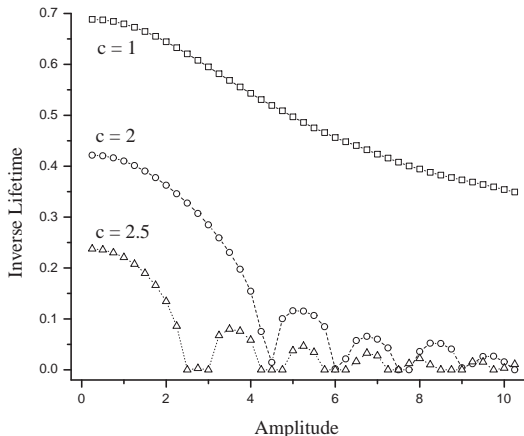


FIG. 4: The decay constant  $\tau^{-1}$  as a function of the initial amplitude of oscillation in the full field theory for  $c = 1$  (solid line), 2 (dashed line), 2.5 (dotted line). Here too we observe bands of stability though none occur for  $c = 1$ .

where

$$\bar{X}(0, x) = \sqrt{1 + 2U(A)} X(0, x) \quad (32)$$

The factor of  $1 + 2U(A)$  arises since, as seen in eq. (29), the external potential contributes to the width of the kink. On evolution the amplitude of oscillations is expected to decay due to radiation. However, the decay is very slow and we can easily track the evolution of the fields through several tens of oscillations with the amplitude of oscillation nearly constant. Another feature worth pointing out is that the angular frequency of oscillations depends on the amplitude of oscillation. The angular frequencies of the runs with large initial amplitudes are  $\sim 1/A$  but at small amplitudes the angular frequency saturates at  $\sim 0.3$ .

Next we ran our numerical code with a non-vanishing perturbation. The initial condition for  $\phi_1$  is still given by eq. (31) but  $\phi_2$  is chosen to be given by

$$\phi_2(t = 0, x) = \epsilon \operatorname{sech}(\bar{X}(0, x)) \quad (33)$$

where  $\epsilon$  is a very small number. The numerical analysis is done with fixed external potential.

As in the linearized analysis, a plot of  $\phi_2(t, x)$  versus time either shows exponential growth (superposed on oscillations), or only oscillations. This allows us to calculate the rate of growth of the perturbations. Once again we find bands of stability (see Fig. 4). The new feature is that these bands occur even for rather large amplitudes showing that dynamical (and not only “jittering”) embedded kinks can be stable. Note that stability bands do not occur in the  $U(1)$  model ( $c = 1$ ) just as in the linearized analysis.

#### IV. CONCLUSIONS AND DISCUSSION

Our analysis of the dynamical embedded kink has shown that there are stability bands in field theories, similar to those for the Mathieu equation. This means that for certain dynamics the embedded kink is stable to perturbations. In these cases, the decay of the embedded kink is determined by the rate of radiation and hence its lifetime can be much longer than the lifetime determined by considering the decay of a static embedded kink.

It is worth commenting on the differences between the linearized and full field theory approaches since the results are quite different. In the linearized case, the oscillating background is inserted by hand and this gives stability bands occurring when the kink has the largest acceleration. In the full field theory, an external potential is imposed, supposedly arising from an external field. Now the kink oscillates naturally, but we observe stability bands at large amplitudes. This feature is explained by our earlier remark that the external potential influences the structure of the kink. As the kink gets further away from the center of attraction, it gets thinner and hence more stable. (The connection between the width of a static kink and the instability eigenvalue can be derived quite easily from a generalization of the solution in eq. (15) as given in Ref. [1].) Then the reason why kinks with large oscillation amplitudes show more stability is that they spend more time in regions where the kink is thin and relatively stable. This is in addition to the effect described in the introduction: the unstable mode moves in and out of the kink, and can grow only while it lies within the kink. Yet the novel feature of stability and instability bands must still be understood in terms of resonance between the oscillation frequency and the phase of the unstable mode when it enters the kink.

A natural question at this point is – can the tension forces that cause extended defects such as domain walls and strings to oscillate be described by an external potential of the type we have used? The answer is in the negative, since the tension forces do not cause changes in the thickness of the defects. The only reason for the defect thickness to change is due to Lorentz contraction. This is our reason for believing that an extended defect will be more accurately described by the linearized analysis of the previous section and not by the full field theory analysis. We are currently extending our analysis to higher dimensions with the aim of studying extended defects.

In the particle physics context, the results are most relevant for the Z-string solutions in the standard model of the electroweak interactions. In 1977 Nambu [7] had estimated the lifetime of segments of Z-string (“dumbbells”) by calculating the electromagnetic emission from the magnetic monopoles at the ends of a rotating dumbbell. If, however, we have a closed loop of Z-string, there are no magnetic monopoles that can lose energy by emitting electromagnetic radiation and the only decay processes are by radiation of massive Higgs and gauge

bosons, and by the structural instabilities of the Z-string discussed in Ref. [8]. (These may be understood in terms of W-condensation [9] in a Z magnetic field background [10, 11, 12, 13].) If we assume that the Z-string in 3+1 dimensions also exhibits stability bands, it would mean that the lifetime of certain Z-string loops may be determined by their radiation rate [14] and not by the instability growth rate of a static Z-string. This would yield a much longer lifetime and would open the possibility that Z-string loops might be produced in future accelerator experiments and might survive long enough to enable detection.

Some cautionary remarks in extrapolating our results to Z-string loops are in order. The Z-string loop is an extended object and if it is to have an extended lifetime, every point on the loop should lie in a stability band. It may even turn out that the Z-string is like the  $c = 1$  embedded kink and that there are no stability bands for any dynamics. Furthermore, the dynamics of the string is due to tension and not due to an external potential. Hence the Z string stability problem could be like the linearized example, in which case only “jittering” Z strings might be stable. The Z string loop can also have angular momentum and this will be an important factor in its evolution. (The stability of spinning string solutions has been studied in [16].) Hence we feel that it is important to directly investigate the lifetime of Z-string loops, keeping in mind the possibility of stability bands.

### Acknowledgments

This work was supported by DOE grant number DEFG0295ER40898 at CWRU.

### APPENDIX A

The following derivation was motivated by Ince’s derivation of Floquet’s Theorem [15]. Consider a dif-

ferential equation of the form:

$$\ddot{\phi} + F(t, x)\phi \equiv H\phi = 0. \quad (\text{A1})$$

If  $H$  is Hermitian over an  $N$  dimensional Hilbert space, we can expand this as:

$$H\phi = \sum_{i=1}^N \lambda_i \phi_i(t, x) = 0 \quad (\text{A2})$$

where the  $\phi_i$  span the Hilbert space. Now, if  $F(t, x) = F(t + T, x)$  where  $T = 2\pi/\omega$  in the notation of the earlier sections, then for each solution  $\phi_i(t, x)$ , there is a solution  $\phi_i(t + T, x)$  by the symmetry in  $H$ . Since the  $\phi_i$  are complete,

$$\phi_i(t + T, x) = \sum_{j=1}^N a_{ij} \phi_j(t, x). \quad (\text{A3})$$

Denoting the matrix  $[a_{ij}]$  by  $\mathcal{A}$  and the  $N \times N$  identity matrix by  $\mathbf{1}_N$ , for each non-degenerate root  $s_i$  of the characteristic equation

$$\det(\mathcal{A} - s\mathbf{1}_N) = 0 \quad (\text{A4})$$

we can construct a basis  $\psi_i$  from the  $\phi_i$  such that

$$\psi_i(t + T, x) = s_i \psi_i(t, x). \quad (\text{A5})$$

Multiplying both sides of the above result by  $e^{-i\nu_i(t+T)}$ , we see

$$e^{-i\nu_i(t+T)} \psi_i(t + T, x) = s_i e^{-i\nu_i T} [e^{-i\nu_i t} \psi_i(t, x)]. \quad (\text{A6})$$

Then it is clear that  $e^{-i\nu_i t} \psi_i(t, x)$  is periodic in  $t$  with period  $T$  if  $s_i = e^{+i\nu_i T}$ . Therefore, solutions of the form

$$\psi_i(t, x) = e^{i\nu_i t} P(t, x) \quad (\text{A7})$$

exist to the equation  $H\psi_i = 0$  with  $P(t + T, x) = P(t, x)$  and  $\nu_i$  given by  $e^{+i\nu_i T} = s_i$  for non-degenerate  $s_i$ .

- 
- [1] P. Morse and H. Feshbach, “Methods of Theoretical Physics”, Vol. 1, McGraw-Hill, New York (1953).
  - [2] T. Vachaspati and M. Barriola, Phys. Rev. Lett. **69**, 1867 (1992).
  - [3] M. Barriola, T. Vachaspati and M. Bucher, Phys. Rev. **D50**, 2819 (1994).
  - [4] T. Vachaspati, Phys. Rev. Lett. **68**, 1977 (1992); **69**, 216E (1992).
  - [5] A. Achúcarro and T. Vachaspati, Phys. Rep. **327**, 347 (1999).
  - [6] R. Rajaraman, “Solitons and Instantons”, Chapter 2, North Holland, Amsterdam (1987).
  - [7] Y. Nambu, Nucl. Phys. **B130**, 505 (1977).
  - [8] M. James, L. Perivolaropoulos and T. Vachaspati, Nucl. Phys. **B395**, 534 (1993).
  - [9] J. Ambjorn and P. Olesen, Int. J. Mod. Phys. **A5**, 4525 (1990).
  - [10] W.B. Perkins, Phys. Rev. **D47**, R5224 (1993).
  - [11] T. Vachaspati, Nucl. Phys. **B397**, 648 (1993).
  - [12] T. Vachaspati, in Proceedings of the NATO workshop on “Electroweak Physics and the Early Universe”, eds. J.C. Romao and F. Friere, Sintra, Portugal (1994), Series B: Physics Vol. 338, Plenum Press, New York (1994).
  - [13] A. Achúcarro, K. Kuijken, L. Perivolaropoulos and T. Vachaspati, Nucl. Phys. **B388**, 435 (1992).
  - [14] T. Vachaspati, A.E. Everett and A. Vilenkin, Phys. Rev. **D30**, 2046 (1984).
  - [15] E. Ince, “Ordinary Differential Equations”, Chapter 15, Dover Publications, New York, (1944).
  - [16] L. Perivolaropoulos, Phys. Rev. **D50**, 962 (1994).